

# Corroborating the inside-out formation of disk galaxies at $z \approx 1$ through detailed decomposition of their UV and H $\alpha$ emission spectra

Connor Streeter

*Department of Physics, The College of Wooster, Wooster, Ohio 44691, USA*

(Dated: May 21, 2022)

This experiment aimed to confirm the theorized inside-out formation of disk galaxies using data collected by the Hubble Space Telescope in the CANDELS and HDUV surveys. The galaxies were analyzed in both the near-infrared (H $\alpha$ ) and ultraviolet (UV) range. The galaxies were modeled using GALFIT’s Sérsic profile in order to extract the emitted UV and H $\alpha$  flux and effective (half-light) radii. The linear growth of the ratio of the UV flux to the near-infrared flux with distance from the galactic centers suggests that younger stars are more frequently located at the outskirts of disk galaxies, which is in agreement with the inside-out formation theory.

## I. INTRODUCTION

Galaxy morphology is a field of study that is not yet fully understood. [1] In order to determine the composition of galaxies, as well as how they evolve over time, it is necessary to understand how they are formed. The current leading theory is that galaxies form from the inside-out rather than the outside-in, meaning that stars first form in what will eventually become the center, and over time more stars begin forming radially outward from that center. [2–4] If the inside-out theory is correct, we would expect to see primarily older stars in the centers of galaxies, while younger stars should be limited to the outer regions.

The Hubble Space Telescope (HST) has been an essential tool in the process of learning how galaxies develop over time. Surveys have been conducted across a broad range of wavelengths, from the near-infrared (H $\alpha$ ) to the ultraviolet (UV). Two of the biggest Hubble projects are the Cosmic Assembly Near-infrared Deep Extragalactic Legacy Survey (CANDELS) and the Hubble Deep UV Legacy Survey (HDUV), both of which consist of hundreds of orbits of HST data, and were used in this experiment. [5–7] The galaxies in these HST images are primarily disk galaxies located at redshifts of  $z = 0.8 - 1.2$ , where the redshift is defined as the ratio of the difference between the observed and emitted wavelengths to the emitted wavelength,  $z = (\lambda_{\text{obs}} - \lambda_{\text{emit}})/\lambda_{\text{emit}}$ . A redshift of  $z = 1$  describes an observed wavelength that is twice as long as the emitted wavelength, which corresponds to light emitted about 8 billion years ago. This was a time of peak star formation in the universe, making it optimal for observing galactic evolution. [1, 8]

Understanding where star formation takes place in galaxies is important because it affects the structural properties of the galaxies that we see today. This, in addition to the sizes of the galaxies as seen in the UV and near-infrared ranges, can be measured using programs such as GALFIT [9, 10] to analyze the HST images. GALFIT extracts information about the objects

in an astronomical image by using parametric functions to model the object in two dimensions. This allows us to confirm whether or not galaxies form from the inside-out, which ultimately should lead us to discover how galaxies grow over time.

## II. THEORY

### Inside-Out Formation

The inside-out theory of galaxy formation tells us that the centers of galaxies at  $z \approx 1$  should contain mostly older stars. Older stars are typically red giants that have evolved off of the main sequence by fusing all of the hydrogen in their core to helium. Once the star runs out of nuclear fuel, its core contracts, and the outer layers rapidly expand. This causes the effective (surface) temperature of the star plummet, so the emitted light is primarily in the infrared spectrum, or close to it. [1, 11] This follows from Wien’s displacement law, which states that the peak wavelength of light emitted by a blackbody is inversely proportional to its temperature. It turns out that the H $\alpha$  emission line, which is near-infrared at a wavelength of 656.3 nm, is the brightest in the hydrogen line making it optimal for observing many celestial objects. [2] If old stars really are located in the central regions of the galaxies, then we should measure higher fluxes in the near-infrared range there, and lower ones in the outer parts of the galaxies. To do this, we define the effective (or half-light) radius  $r_e$  as the radial distance from the galactic center to the point where half of the total light being emitted by the galaxy is contained. If the inside-out theory is correct, the H $\alpha$  line should be brighter at distances  $r < r_e$  and dimmer at distances  $r > r_e$ .

One issue with observing disk galaxies at  $z \approx 1$  is that there is a large amount of interstellar gas and dust located in these galaxies, as stars are only beginning to form. Dust in particular causes a reddening effect in some instances, which is extremely difficult to account

for with imaging tools such as GALFIT. [9] This can lead to incorrect values for the magnitude, and thus the flux, of the galaxies in the infrared range. For this reason, I decided to analyze the galaxies in the ultraviolet (UV) range of the spectrum in addition to the near-infrared so that the results may be compared for accuracy. Highly massive stars such as blue giants and supergiants are much hotter than red giants, which causes them to emit large amounts of UV radiation - again due to Wien's law. These massive stars exhaust their hydrogen fuel much faster than main sequence stars due to their extreme temperatures and therefore have much shorter lifetimes than red giants, typically on the scale of millions rather than billions of years. This means that blue giants must be relatively young compared to most stars [12]. If the UV flux is higher at distances  $r > r_e$ , it would suggest that younger stars are located on the outskirts of disk galaxies and thus support the inside-out formation theory.

### The Sérsic Profile

One of the main functions used in modeling the light distribution of galaxies is the Sérsic profile, which gives the intensity (brightness) of a galaxy as a function of radial distance from the center as shown in Fig. 1. GALFIT is able to fit galaxies with the Sérsic profile to find the surface brightness in pixels. [9] This form of the Sérsic profile is given by

$$\Sigma(r) = \Sigma_e \exp \left[ -\kappa \left( \left( \frac{r}{r_e} \right)^{1/n} - 1 \right) \right], \quad (1)$$

where  $\Sigma_e$  is the pixel surface brightness at the effective radius  $r_e$  and  $\kappa$  is a parameter depending on the Sérsic index  $n$ , which depends on the size and light intensity of the galaxy. Higher mass galaxies such as ellipticals tend to have higher concentrations of light in the central regions (and thus a larger Sérsic index) while disk (spiral) galaxies typically have lower concentrations of light in the center (and thus a smaller Sérsic index). [2] The Sérsic profile is actually a generalized version of the classic de Vaucouleurs profile, which is known to be a good approximation of elliptical galaxies and occurs when  $n = 4$ . Disk galaxies are usually best approximated by indices of  $n \approx 1$ , which is another special case of the Sérsic profile known as the exponential profile. [9][10]

The integrated flux as  $r \rightarrow \infty$  for an object fit by the Sérsic profile is

$$F_{\text{tot}} = 2\pi r_e^2 \Sigma_e e^\kappa n \kappa^{-2n} \Gamma(2n) q / R(C_0; m), \quad (2)$$

where  $\Gamma(2n)$  is the gamma function,  $q$  is the axis ratio of the galaxy (semi-minor over semi-major axis), and  $R(C_0; m_i)$  is a correction factor for the deviation of the galaxy from a perfect ellipse. The constant  $m$  is the

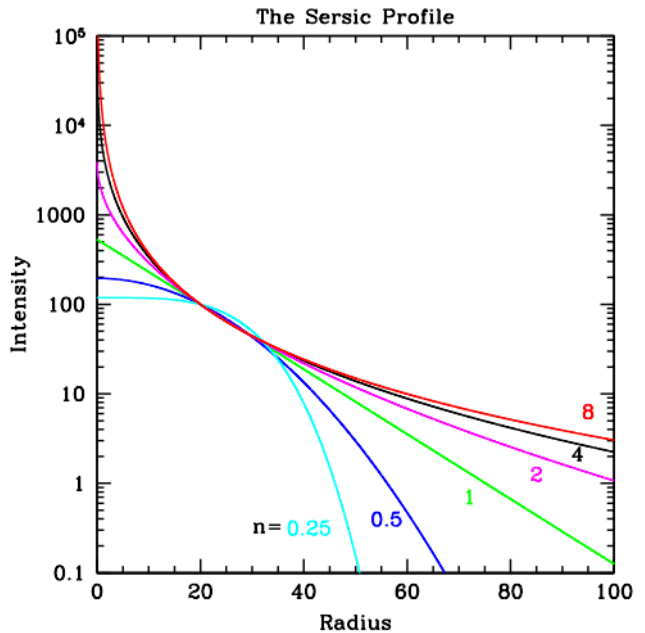


FIG. 1: The Sérsic profile is often used to study galaxy morphology, and gives the intensity of a galaxy as a function of its radius. Sérsic indices ranging from  $n = 0.25$  to  $n = 8$  are shown here (from [9]).

number of Fourier modes and  $R(C_0)$  is a function of the parameter  $C_0$  that depends on the beta function in a complicated way.

GALFIT is capable of estimating  $R(C_0; m)$  if the position angle is known. The position angle, along with the axis ratio and half-light radius, are known features of the galaxy, which means that the total integrated flux can be found by GALFIT upon inputting these variables. [9] The actual brightness of the galaxy is known as the total integrated magnitude, and is given by

$$m_{\text{tot}} = -2.5 \log_{10} \left( \frac{F_{\text{tot}}}{t_{\text{exp}}} \right) + \text{mag zpt}, \quad (3)$$

where  $t_{\text{exp}}$  is the EXPTIME - essentially the time it takes for the GALFIT algorithm to run, and the magnitude zeropoint (mag zpt) is the magnitude of an object producing one count per second on the detector [10]. The photometric magnitude zero point is 26.563 for the CANDELS survey and 24.087 for HDUV. [5][7]

### III. PROCEDURE

The main purpose of this experiment was to confirm the inside-out formation of disk galaxies by analyzing the flux emitted from them. The flux was measured in both the  $H\alpha$  and UV spectrum by considering data collected from two different Hubble Space Telescope



FIG. 2: An example GALFIT output file. The original image is on the left, the modeled objects are in the middle, and the residual background light is on the right.

(HST) surveys. The survey used to analyze galaxies in the  $H\alpha$  line was the Cosmic Assembly Near-infrared Deep Extragalactic Legacy Survey (CANDELS), while the Hubble Deep UV Legacy Survey (HDUV) was used to analyze galaxies in the ultraviolet spectrum. The data from both of these surveys is publicly available for free online, and consists of images taken from hundreds of orbits of the HST. These images were opened and edited using the program SAOImageDS9 (DS9). [13]

In order to analyze the images and extract information about the galaxies, I made use of GALFIT to fit functions to the images. The primary function I used was the Sérsic profile, which was used to determine how the flux of the galaxies varies from different distances to their centers. I also made use of the background sky function, which removes the excess light from objects in the image other than the galaxy being fit by the Sérsic function. This results in an output file containing three distinct images: the initial, unmodified image, an image of just the galaxy being analyzed, and an image of the background light that was removed by the sky function. An example output file is shown in Fig. 2.

I have previously conducted research on galaxies in the infrared spectrum using GALFIT, so I used that source code as the basis for analysis of the galaxies in the CANDELS survey. The program can be modified to output many variables, but the ones I focused on were the magnitude  $m_{\text{tot}}$ , effective radius  $r_e$ , position angle  $\theta$ , and axis ratio  $q$  of the galaxy. The flux of the galaxy can be calculated if the magnitude is known using Eq. (3). I wanted to find the flux at different distances from the center, including  $r_e/2$ ,  $r_e$ , and  $2r_e$ . GALFIT determines  $r_e$  through pixel data and gives the magnitude of the galaxy at  $r_e$ . I attempted to modify the code to give the magnitude at the other two distances, but unfortunately was not able to accurately do so, which was probably the most disappointing part of the experiment.

Additionally, I analyzed the flux of the galaxies in the UV range using images collected from the HDUV survey. One major issue in this process was galaxy identification. Unfortunately, CANDELS and HDUV did not use the same numbering process for identifying galaxies, which resulted in much difficulty in finding the corresponding galaxies in the HDUV survey. Once a galaxy had been identified for analysis in the CANDELS survey, I had to search for the corresponding galaxy in the source catalogue for HDUV. This process was eventually made feasible through the use of software known as TOPCAT [14], which is a graphical viewer for tabular data that assists in the manipulation of the source catalogues used to identify the galaxies. This then allowed me to run GALFIT on specific galaxies through the lens of both the CANDELS and HDUV surveys. I ultimately ended up analyzing 16 different galaxies, and found their  $H\alpha$  and UV fluxes at the effective radii in both ranges of the electromagnetic spectrum.

#### IV. RESULTS & ANALYSIS

The half-light radii and magnitudes for 16 different disk galaxies in both the  $H\alpha$  and UV spectra were determined using GALFIT. The relationship between the half-light radii is shown in Fig. 3.

The slope of this line is  $2.1 \pm 0.2$  meaning that the UV  $r_e$  is approximately twice as large as the  $H\alpha$   $r_e$ . This is consistent with the inside-out formation theory for disk galaxies because it shows that the galaxies are emitting more UV light as the distance from the center increases, which is caused by the younger stars that are forming in the outer regions.

The other relationship that I analyzed was the flux

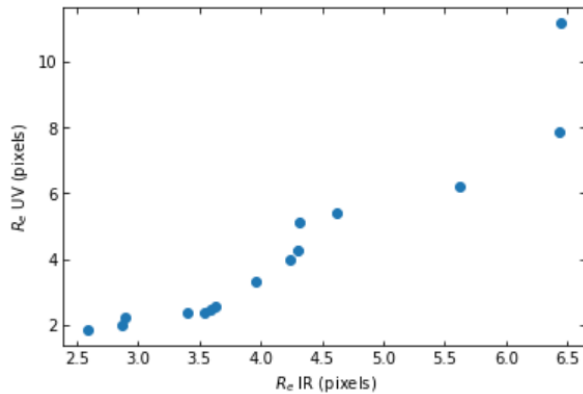


FIG. 3: Plot of the effective radii in the UV range against the corresponding effective radii in the near-infrared. The UV radii become larger as the distances increased.

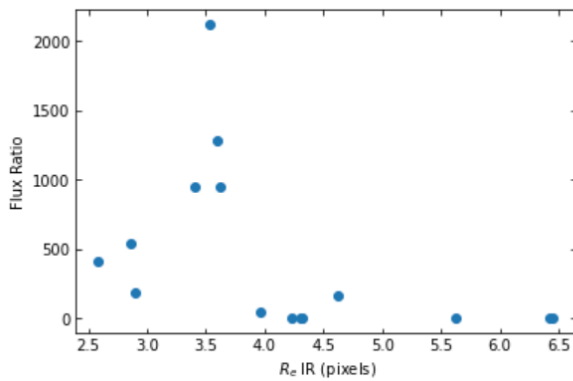


FIG. 4: Plot of the the flux ratio against  $r_e$  in the  $H\alpha$  spectrum.

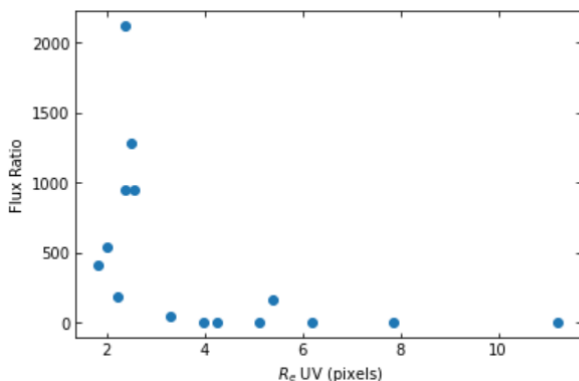


FIG. 5: Plot of the flux ratio against  $r_e$  in the UV spectrum.

ratio against the half-light radius in both the near-infrared and UV spectra, as shown in Figs. 4 and Fig5, respectively. Figs. 4 and 5 appear somewhat similar,

which is not what the theory predicted. If we consider the IR  $r_e$ , the flux ratio should increase at first and then gradually decrease, as it does in Fig. (4), however, this should not be the case if we consider the UV  $r_e$ . In fact, we should observe the exact opposite trend. One possible explanation for this is that the GALFIT program that was written did not correctly identify the effective radius for the galaxies in the HDUV images. The amount of flux emitted by the galaxies in the near-infrared spectrum was significantly higher than the amount of UV flux, with over 95% of the total flux being in the IR range. This means that the UV data was overshadowed by the IR data, which could explain why the UV  $r_e$  results were similar to that for the IR  $r_e$ .

## V. CONCLUSION

Unfortunately, I was not able to plot the flux ratio at the three different distances as I had originally intended, but I was still able to find evidence that disk galaxies form from the inside-out. The primary evidence for this was the plot of the effective radius in the UV range against the  $H\alpha$   $r_e$ , which was somewhat linear. This supports the inside-out theory of galaxy formation because it is an example of more UV light (and less near-infrared light) being emitted as the distance from the center of the galaxy increases. This was corroborated with the plot comparing the flux ratio to the IR  $r_e$ , which also demonstrated the same thing. Higher UV fluxes are emitted by young stars meaning that we can conclude star formation rates in disk galaxies get higher as distances from the center increase. The discrepancy with the final plot was very likely due to the large amount of near-IR flux being emitted and thus is not necessarily evidence against inside-out formation.

One potential aspect that could be explored in future research is the mass of the galaxies, which is hypothesized to affect how formation occurs. [15, 16] Higher mass galaxies such as large ellipticals are thought to form a bit differently from regular galaxies. Since the two surveys used in this project consisted almost exclusively of low to medium mass disk galaxies, another survey such as the 3D-HST grism survey could be used to investigate the higher mass galaxies and see whether or not they form inside-out.

## VI. ACKNOWLEDGMENTS

I would like to thank Dr. Manz and Dr. DeGroot for providing advice and assistance with various things throughout the course of the project.

- 
- [1] Carroll, B. & Ostlie, D. *An Introduction to Modern Astrophysics* (Addison-Wesley, 2006), 2nd edn.
- [2] Nelson, E. J. *et al.* Spatially Resolved H $\alpha$  Maps and Sizes of 57 Strongly Star-forming Galaxies at  $z \approx 1$  from 3D-HST: Evidence for Rapid Inside-out Assembly of Disk Galaxies. *The Astrophysical Journal* **747**, L28 (2012). URL <https://doi.org/10.1088/2041-8205/747/2/L28>.
- [3] Nelson, E. J. *et al.* The Radial Distribution of Star Formation in Galaxies at  $z \approx 1$  from the 3D-HST Survey. *The Astrophysical Journal* **763**, L16 (2013).
- [4] Nelson, E. J. *et al.* Where Stars Form: Inside-out Growth and Coherent Star Formation from HST H $\alpha$  Maps of 3200 Galaxies across the Main Sequence at  $0.7 < z < 1.5$ . *The Astrophysical Journal* **828**, 27 (2016).
- [5] Grogin, N. A. *et al.* CANDELS: THE COSMIC ASSEMBLY NEAR-INFRARED DEEP EXTRAGALACTIC LEGACY SURVEY. *The Astrophysical Journal Supplement Series* **197**, 35 (2011).
- [6] Koekemoer, A. M. *et al.* CANDELS: The Cosmic Assembly Near-infrared Deep Extragalactic Legacy Survey—The Hubble Space Telescope Observations, Imaging Data Products, and Mosaics. *The Astrophysical Journal Supplement Series* **197**, 36 (2011).
- [7] Oesch, P. A. *et al.* HDUV: The Hubble Deep UV Legacy Survey. *The Astrophysical Journal Supplement Series* **237**, 12 (2018).
- [8] Maoz, D. *Astrophysics in a Nutshell* (Princeton University Press, 2016), 2nd edn.
- [9] Peng, C. Y., Ho, L. C., Impey, C. D. & Rix, H.-W. Detailed Structural Decomposition of Galaxy Images. *The Astronomical Journal* **124**, 266–293 (2002).
- [10] Peng, C. Y., Ho, L. C., Impey, C. D. & Rix, H.-W. Detailed Decomposition of Galaxy Images. II. Beyond Axisymmetric Models. *The Astronomical Journal* **139**, 2097–2129 (2010).
- [11] Choudhuri, A. R. *Astrophysics for Physicists* (Cambridge University Press, 2010), 1st edn.
- [12] Ryden, B. & Peterson, B. M. *Foundations of Astrophysics* (Cambridge University Press, 2020), 1st edn.
- [13] for Astrophysics, H. . S. C. SAOImageDS9: An image display and visualization tool for astronomical data. (2022).
- [14] Taylor, M. TOPCAT: Tool for Operations on Catalogues and Tables. (2022).
- [15] Brammer, G. B. *et al.* 3D-HST: A Wide-field Grism Spectroscopic Survey with the Hubble Space Telescope. *The Astrophysical Journal* **200** (2012).
- [16] Nelson, E. J. *et al.* Spatially resolved star formation and inside-out quenching in the TNG50 simulation and 3D-HST observations. *Monthly Notices of the Royal Astronomical Society* **508**, 219–235 (2021).